Microbiological Research 265 (2022) 127200

Contents lists available at ScienceDirect

Microbiological Research

journal homepage: www.elsevier.com/locate/micres

Antifungal activity of vitamin D_3 against *Candida albicans in vitro* and *in vivo*

Junwen Lei [a], Wei Xiao [a], Jinping Zhang [a], Fangyan Liu [a], Caiyan Xin [a], Bo Zhou [b], Wenbi Chen [a,*], Zhangyong Song [a,*]

[a] *The Platform of Molecular Biotechnology, Public Center of Experimental Technology, School of Basic Medical Sciences, Southwest Medical University, Luzhou 646000, People's Republic of China*

[b] *Huangdao District of Traditional Chinese Medicine, Qingdao 266500, China*

ARTICLE INFO

Keywords:
Vitamin D_3
Candida intra-abdominal
Candidiasis
Ribosome
Coenzyme

ABSTRACT

The incidence of intra-abdominal candidiasis (IAC), characterized by high morbidity and mortality, has become a serious concern. The limitations of current antifungal drugs on the market underscores the importance of the development of novel antifungal agents. In the present study, the antifungal activity of vitamin D_3 (VD_3) against various *Candida* species was investigated. *In vitro*, the broth microdilution method and solid plate assay confirmed that VD_3 inhibited the growth of *Candida* spp. in a broad-spectrum, dose-dependent manner. VD_3 also had a significant antifungal effect on the initiation, development, and maturation phases of biofilm formation in *Candida albicans*. The mechanism of VD_3 action was explored by transcriptomics and reverse transcription quantitative PCR (RT-qPCR) analysis, and showed that VD_3 affects ribosome biogenesis, coenzyme metabolism, and carbon metabolism. These results suggested that VD_3 may have multitarget effects against *C. albicans*. In the murine IAC model, VD_3 reduced the fungal burden in the liver, kidneys, and small intestine. Further histopathological analysis and quantification of plasma cytokine levels confirmed that VD_3 treatment significantly decreased the infiltration of inflammatory cells and the levels of plasma interferon (IFN)-γ and tumor necrosis factor (TNF)-α. Taken together, these findings suggest a new antifungal mechanism for VD_3 and indicate that VD_3 could be an effective therapeutic agent for use in IAC treatment.

1. Introduction

Candida albicans mainly colonizes the oral cavity (Jiang et al., 2020), the upper respiratory tract (Pappas et al., 2009), the intestinal tract (Kumamoto et al., 2020), and the vagina (Cauchie et al., 2017), and can cause mucosal and invasive infection. Invasive, systemic *Candida* infections are life-threatening for patients, especially immunosuppressed patients. Treatment of invasive candidiasis is more difficult than mucosal candidiasis, especially when *Candida* species have invaded the brain and kidneys (Andes, 2019). In the past few years, an increasing rate of invasive fungal infection has been a major reason for the low cure rate in intensive-care units (ICUs) (Bassetti et al., 2017; Pappas et al., 2018). The incidence of systemic candidiasis and intra-abdominal candidiasis (IAC) among these invasive fungal infections in ICUs rank first and second, respectively (Bassetti et al., 2015; Montravers et al., 2015), with the mortality rate of invasive candidiasis in ICUs being 40 − 55% (Logan et al., 2020). Several factors (such as advanced medical technology, widespread use of antibiotics, long-term ICU stay, invasive surgery, and the use of catheters) are linked to the emergence of invasive candidiasis (Bassetti et al., 2017), while the ability of *C. albicans* to form biofilms exacerbates the infection and complicates treatment (Nobile and Johnson, 2015).

Nowadays, three available classes of agents (azoles, echinocandins, and polyenes) are used to treat invasive candidiasis. However, the emergence of drug-resistance *C. albicans* has become a major challenge in clinical work (Lee et al., 2021; Zhang et al., 2021). Additionally, the prevalence of other drug-resistant *Candida* species (such as *C. glabrata* and *C. auris*) and the complexity of critical patients require more specific therapy (Andes, 2019). Against this grim backdrop, the development of novel antifungal agents has become an urgent requirement. Unfortunately, the speed of the development and registration of effective new antifungal drugs cannot meet the current demands (Thangamani et al., 2017). Nonetheless, drug repositioning has become a feasible strategy to accelerate the development of new drugs (Andreani et al., 2020; Avram

* Corresponding authors.
E-mail addresses: leijunwen0519@163.com (J. Lei), shawn156@163.com (W. Xiao), zhangjpwcx@163.com (J. Zhang), liufangyan1989@163.com (F. Liu), xincy0211@126.com (C. Xin), 115492918@qq.com (B. Zhou), cwb298@163.com (W. Chen), szy83529@163.com (Z. Song).

https://doi.org/10.1016/j.micres.2022.127200
Received 4 April 2022; Received in revised form 4 August 2022; Accepted 13 September 2022
Available online 20 September 2022

et al., 2021). Here, we describe an alternative strategy by studying the antifungal effects and mode of action of an existing drug on the market, namely vitamin D_3 (VD_3).

VD_3 is a pluripotent hormone, and its classical biological effect is to treat vitamin D deficiency and rickets. It is produced in the skin after being exposed to the sun or is obtained from food (Christakos et al., 2019). In recent years, the extra-skeletal biological effects of VD_3 have attracted much attention, especially its roles in the antitumor (Carlberg and Munoz, 2022; Christakos et al., 2016), immunity (Meza-Meza et al., 2020; Mora et al., 2008), and anti-infection responses (Hu et al., 2019). In this manuscript, we focus on the antifungal role of VD_3. Previous investigations found that infection by *Aspergillus fumigatus* enhances the levels of antimicrobial peptides by increasing the concentration of active vitamin D_3 in 16HBE cells (Li et al., 2015). Moreover, a VD_3-deficient diet aggravated inflammation and caused changes in local immunity in the *A. fumigatus* mouse model of chronic rhinosinusitis (Mulligan et al., 2017), whereas daily vitamin D_3 supplementation markedly reduced IL-13 response and IgE levels as well as increasing the serum vitamin D_3 level (Nguyen et al., 2015). In addition, VD_3 reduced the levels of pro-inflammatory cytokines (IFN-γ, IL-6, IL-17, and TNF-α) and inhibited the Dectin-1, Toll-like receptor (TLR) 2, TLR 4, and mannose receptors during *C. albicans* infection (Khoo et al., 2011). Moreover, *in vitro*, VD_3 has a direct antifungal effect on *C. albicans* (Bouzid et al., 2017). Despite all this information, the direct antifungal mechanism of VD_3 against *C. albicans* is still unclear; more importantly, the antifungal effect of VD_3 in treating IAC *in vivo* has not yet been explored.

In this study, we evaluated the antifungal activity of VD_3 on various *Candida* spp., namely *C. albicans*, *C. glabrata*, *C. krusei*, *C. parapsilosis*, and *C. tropicalis*, and revealed that VD_3 directly inhibits hyphal growth and blocks biofilm formation. In addition, fungal hydrophobicity was reduced after treatment with VD_3. Furthermore, RNA sequencing (RNA-Seq) and reverse transcription quantitative PCR (RT-qPCR) analysis showed that VD_3 impacted carbohydrate metabolism and ribosomal biogenesis, and the anti-candidiasis activity of VD_3 was demonstrated in an IAC mouse model.

2. Materials and methods

2.1. Chemicals, fungal strains, and media

Four standard strains, namely *C. albicans* ATCC MYA-2876, *C. albicans* ATCC 90028, *C. parapsilosis* ATCC 22019, and *C. krusei* ATCC 6258, were purchased from the American Type Culture Collection (ATCC). In addition, five clinical strains, namely two *C. parapsilosis* strains (Cp1 and Cp2), two *C. tropicalis* strains (Ct2 and Ct3), and one *C. glabrata* strain (Cg1), were used in this study. All test strains had previously been identified by sequencing the internal transcribed spacer of nuclear ribosomal DNA. Vitamin D_3 (Macklin, Shanghai, China), RPMI-1640 medium (Hyclone, Chengdu, China), 2,3-bis-(2-methoxy-4-nitro-5-sulfophenyl)− 2 H-tetrazolium-5-carboxanilide (XTT) (Macklin, Shanghai, China) and calcofluor white (Sigma, Shanghai, China) were used in this study.

2.2. Antifungal susceptibility assay

To quantify any broad-spectrum antifungal activity, the broth microdilution assay was carried out according to the document M27-A3 (Thangamani et al., 2017). Briefly, the VD_3 was prepared in dimethyl sulfoxide (DMSO) at a stock solution of 50 mg/mL and then diluted in RPMI-1640 medium (containing 0.05% Tween 80) to 0.0, 0.1, 0.2, 0.6, 0.8, 1.0, 1.2, 1.4, and 1.6 mg/mL with 100 μL of the working solution being pipetted into individual wells of a 96-wells plate. Each strain was separately cultured in yeast extract peptone dextrose (YPD) medium at 37 ℃ with agitation (200 rpm) overnight. To each well, 100 μL of spore suspension was added at a concentration within the range 0.5–2.5 × 10^4 spore cells/mL. Then, the wells were incubated at 37 ℃ for 24 h. The minimum inhibitory concentration (MIC) values that suppressed fungal growth by 90% were determined.

2.3. Time kill assay

In brief, the test strains at a concentration of 5 × 10^5 spore cells/mL were treated with a dilution series of either VD_3 or the anti-candidiasis agent fluconazole in liquid YPD medium and incubated at 37 ℃ in a shaking incubator at 200 rpm (Thangamani et al., 2017). Aliquots of the spore suspensions were collected after incubation at 2, 4, 8, 12, or 24 h, diluted in phosphate buffered saline (PBS) and then spread on to solid YPD agar medium and incubated at 37 ℃ for 24 − 48 h to count fungal colony forming units (CFU).

2.4. Hyphal growth analysis

The hyphal growth analysis was carried out as described previously (Xu et al., 2019). In brief, all test strains were cultured in liquid RPMI-1640 + 10% (v/v) fetal bovine serum (FBS) or on solid YPD + 10% (v/v) FBS agar plates. The fungal cells (10^6 cells/mL) were cultured with 0.4 or 0.8 mg/mL of VD_3 in RPMI-1640 + 10% (v/v) FBS medium at 37 ℃ for 6 h. Hyphal morphology was observed under a light microscope. Meanwhile, the spore cells pre-cultured overnight (10^6 cells/mL) were spotted onto YPD + 10% (v/v) FBS plates containing 0.4 or 0.8 mg/mL of VD_3. After three days of incubation at 37 ℃, the fungal morphologies were recorded using a digital camera.

2.5. Biofilm formation test

To determine the effect of VD_3 on the different developmental stages of biofilm formation, the test strains were assessed using the Crystal Violet (CV) biofilm biomass and XTT tetrazolium salt-based biofilm metabolic activity assays as described previously (Rajendran et al., 2015). Briefly, 200 μL spore suspension in RPMI-1640 liquid medium was transferred to wells on 96-well plates and incubated at 37 ℃ for 90 min, 12 h, or 48 h, to generate the initial, developmental, and maturation phases of biofilm formation, respectively. After the specific time point, each well was washed twice with PBS, then treated with VD_3 for 6 h. Subsequently, cells pre-cultured for 90 min or 12 h continued to be cultured for a total of 48 h, and were then examined; cells pre-cultured for 48 h were examined directly. The biofilm mass and metabolic activity were confirmed by the CV and XTT assays, respectively.

Furthermore, the three-dimensional structure of the *C. albicans* ATCC MYA-2876 biofilm was determined by confocal laser scanning microscopy (Del Rio et al., 2019). Circular microscope cover glasses were seeded into 6-well plates and 3 mL of fungal suspension (10^6 cells/mL) with or without VD_3 were incubated at 37 ℃ for 24 h without shaking. Subsequently, plates were gently washed with PBS and the biofilm was stained with 1 mL of calcofluor white (CFW) at room temperature for 3 min. Then, the biofilm was examined under a confocal laser scanning microscope (TCS-SP8, Leica, Wetzlar, Germany).

2.6. Cell surface hydrophobicity (CSH) assay

The effect of VD_3 on CSH was determined as described previously (Liu et al., 2019). Briefly, fungal cells were cultured in the presence of VD_3 (0.4 or 0.8 mg/mL) at 37 ℃ for 12 h in a shaking incubator at 200 rpm. Then, the cells were harvested and resuspended in 2.45 mL of PBS. The absorbance of a 200 μL aliquot of the suspension was measured as OD_{600} (A_0). Chloroform added to take total volume 3 mL, vortexed for 3 min, and allowed to stand for 30 min. Finally, 200 μL of the upper layer was measured at OD_{600} (A_1). Hydrophobicity index (%)= $(1 - A_1 / A_0) \times 100$.

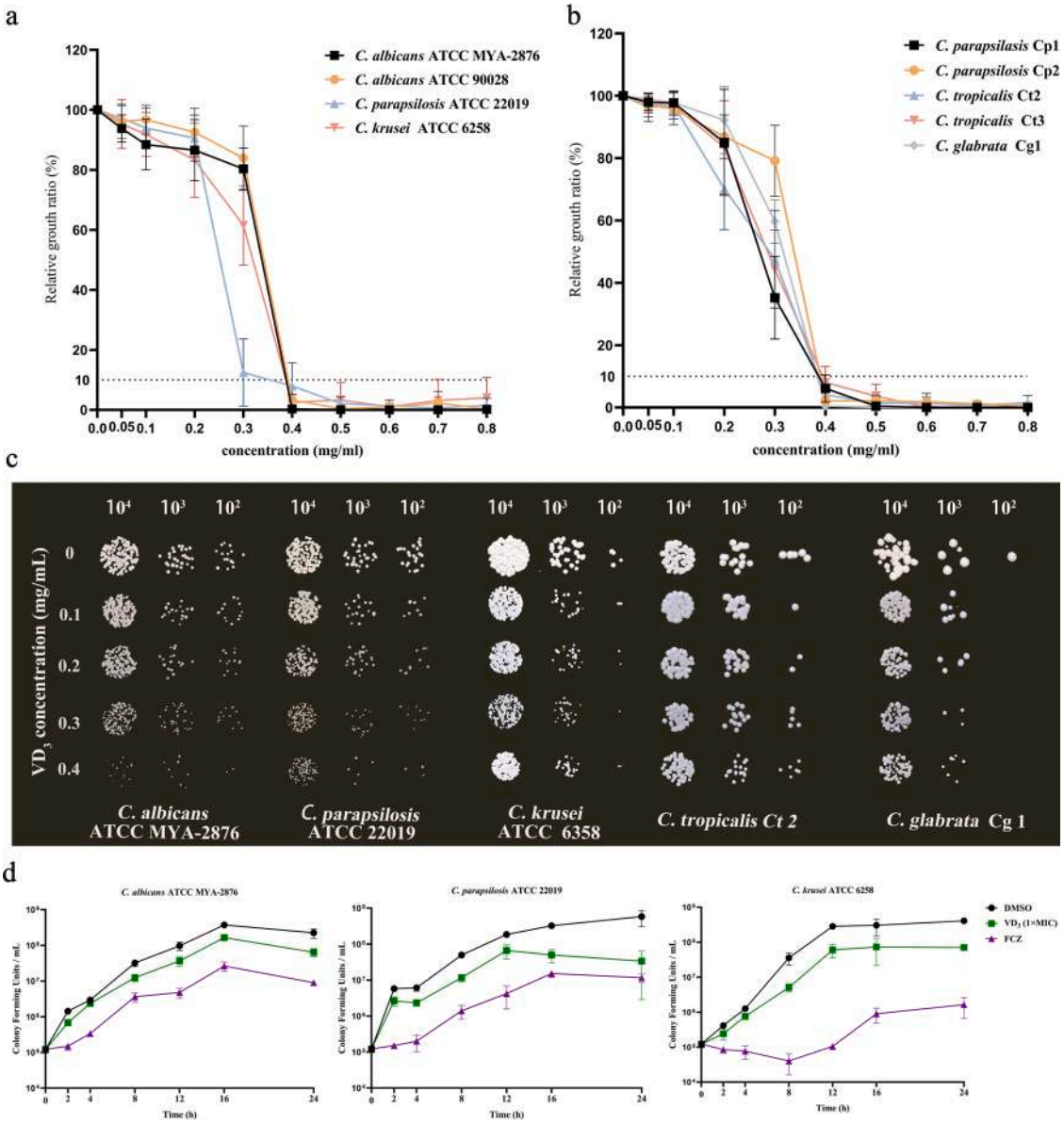

Fig. 1. VD_3 inhibits the growth of *Candida*. (a, b) The relative growth curve of *Candida* species after being treated with various concentrations of VD_3. (c) Effect of VD_3 on growth of the test strains growth. After cultured overnight, strains were spotted onto YPD agar plates (containing 0.0, 0.1, 0.2, 0.3, or 0.4 mg/mL VD_3) and cultured at 37 °C for 2 d. (d) Time-kill curves of VD_3. Three standard strains, including *C. albicans* ATCC MYA-2876, *C. parapsilosis* ATCC 22019 and *C. krusei* ATCC 6258, were treated with MIC of VD_3 and fluconazole (FCZ). Each experiment was carried out with three biological replicates.

2.7. Transcriptomic and RT-qPCR analysis

To investigate the molecular mechanism of the antifungal action of VD_3, *C. albicans* ATCC MYA-2876 cells were inoculated into fresh YPD liquid medium and incubated at 37 ℃, shaking at 200 rpm. The cells were treated with 0.0 or 0.4 mg/mL VD_3 and were collected after 12 h culture for total RNA extraction. RNA-samples and library construction were performed according to the manufacturer's protocols. RNA-Seq was conducted by BioMarker (Beijing, Qingdao, China) using a Novaseq 6000 sequencing platform (Illumina). The detailed methods and gene functional annotation are described in previous reports (Anders and Huber, 2010; Kanehisa et al., 2008). Data were submitted to the Beijing Institute of Genomics Genome Sequence Archive (No. PRJCA007860).

To quantify the transcriptional activity of genes influenced by VD_3 treatment, samples of *C. albicans* ATCC MYA-2876 strain inoculated into the liquid medium at a concentration of 10^6 cells/mL without or with 0.4 mg/mL VD_3 were cultured at 37 ℃ at 200 rpm and collected at 0, 6, or 12 h for total RNA extraction using Yeast Processing Reagent (Takara, Dalian, China). The RNA concentration was measured spectrophotometrically (NanoDrop 2000 spectrophotometer, Thermo Fisher, Shanghai, China). The regents for cDNA reverse transcription and RT-qPCR were supplied by Takara. The transcript of *β-actin* (*ACT1*) gene was used as an internal standard. Primers are shown in Table S1. The $2^{-\Delta\Delta CT}$ method was used to determine any relative change in genes expression (Livak and Schmittgen, 2001).

2.8. In vivo antifungal studies

C57BL/6 J male mice (6- to 8 weeks old; Dossy, Chengdu, China) were assigned to one of five groups. The IAC mouse model was induced by intraperitoneal injection with 100 μL sterile saline containing 10^8 cells/mL of *C. albicans* in all group except for the control group (Lee et al., 2020). The five groups were: (1) The Ca group was treated daily

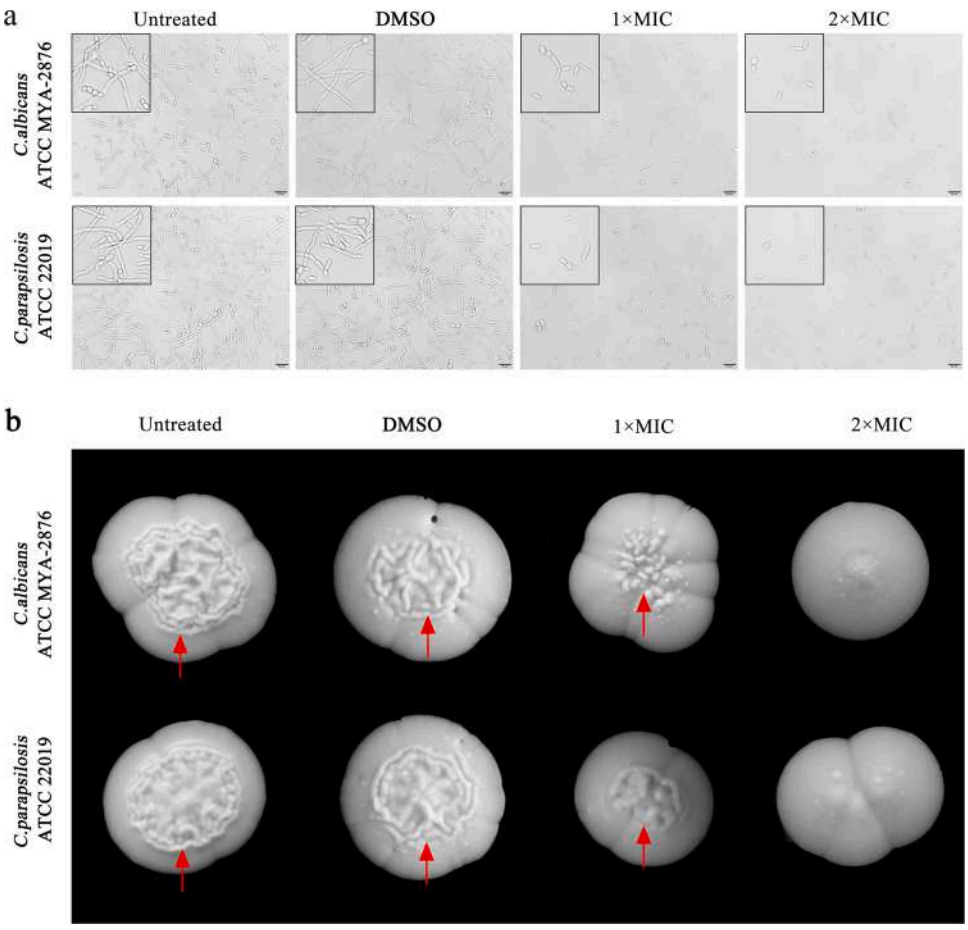

Fig. 2. VD_3 inhibits the hyphal growth of *C. albicans* and *C. parapsilosis*. *C. albicans* and *C. parapsilosis* were incubated in (a) 1640 RPMI + 10% (v/v) FBS liquid medium or on (b) YPD + 10% (v/v) FBS agar medium treated with blank control (untreated), dimethyl sulfoxide (DMSO, 0.8%), 1 ×MIC or 2 ×MIC of VD_3. The uniformly enlarged image is presented in the black boxes on the left-hand panels in (a). The hyphae are indicated by a red arrow on agar medium in (b). Each experiment was carried out with three biological replicates.

with 100 μL sterile saline containing 0.24% of DMSO after 1 h infection with *C. albicans* cells; (2) the 60 μg/kg group was treated daily with 60 μg/kg of VD_3 (diluted in sterile saline containing 0.24% of DMSO) after 1 h infection with *C. albicans* cells; (3) the 600 μg/kg group was treated daily with 600 μg/kg of VD_3 (diluted in sterile saline containing 0.24% of DMSO) after 1 h infection with *C. albicans* cells; (4) the FCZ group was treated with 10 mg/kg of fluconazole after 1 h infection with *C. albicans* cells; and (5) the control group was injected with 100 μL sterile saline and after 1 h later was treated with 100 μL sterile saline (containing 0.24% of DMSO). Treatments were continued for 14 days. Samples of blood, liver, kidney and small intestine were collected on the 3rd and 14th day. Plasma was obtained by centrifugation of blood at 1500 g for 10 min and stored at − 80 ℃. After that, chemokine levels were measured by the Mouse Inflammation Kit (CBA; BD Biosciences, State of New Jersey, USA) using flow cytometry (ACEA NovoCyte™ 2070 R, Harbin, China). One-half of each sample of liver, kidneys and small intestines were removed for fungal burdens. And the other was processed for Periodic Acid-Schiff staining or Hematoxylin-Eosin staining histopathological examination (Chen et al., 2020b).

2.9. Statistical analyses

Each experiment was carried out with independent biological replicates. Statistical analyses were conducted by one-way ANOVA or unpaired t test using GraphPad Prism 9 (GraphPad Software Inc., La Jolla, CA, USA). Statistical significance was defined as $P \leq 0.05$.

3. Results

3.1. In vitro antifungal activity of VD_3 against fungal growth

The relative growth of the four standard strains (Fig. 1a) and the five clinical isolates (Fig. 1b) following treatment with VD_3 concentrations ranging from 0.05 to 0.8 mg/mL showed that VD_3 exhibited significant anti-*Candida* activity, with 90% inhibition of the growth of fungal cells (MIC) being achieved by 0.4 mg/mL VD_3. In particular, the inhibition rate on *C. parapsilosis* ATCC 22019 by 0.3 mg/mL VD_3 was 85.57 ± 11.18%. Furthermore, VD_3 inhibited *Candida* growth in a dose-dependent manner (Fig. 1a-c). The time-kill assay also showed that VD_3 inhibited the growth of three of the standard strains in the lag, logarithmic and stationary phases (Fig. 1d).

To confirm the antifungal activity of VD_3 on hyphal formation, hyphae induced on RPMI-1640 + 10% (v/v) FBS broth medium or YPD + 10% (v/v) FBS agar plates were used. In the broth medium, a large number of hyphae were observed in the untreated and DMSO groups. On the other hand, in the presence of 1 ×MIC or 2 ×MIC of VD_3, hyphal cells were not observed (Fig. 2a). On YPD + 10% (v/v) FBS agar, colonies in the untreated and DMSO groups were wrinkled (red arrow), although, the wrinkled appearance of the colonies was attenuated by treatment with 1 ×MIC of VD_3, with the colonies being completely smooth in response to treatment with 2 ×MIC of VD_3 (Fig. 2b). This indicated that VD_3 inhibits the development of hyphae in a dose-dependent manner.

3.2. VD_3 inhibits biofilm formation

As hyphae are necessary for biofilm formation, the effect of VD_3 on

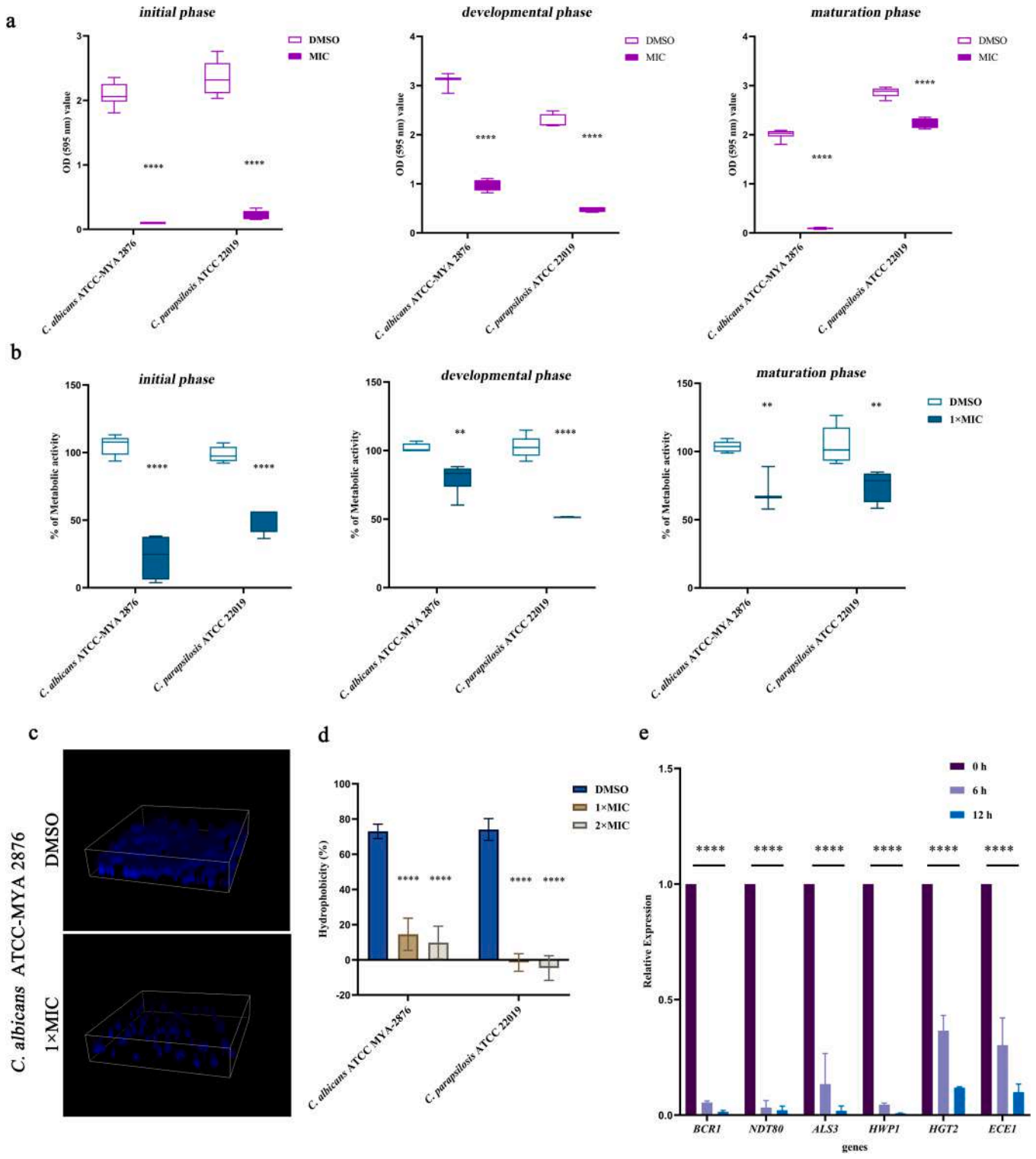

Fig. 3. Effect of VD_3 on biofilm development. Biofilm biomass and metabolic activity were tested by the (a) Crystal Violet (CV) assay and the (b) 2,3-bis-(2-methoxy-4-nitro-5-sulfophenyl)− 2 H-tetrazolium-5-carboxanilide (XTT) assay, respectively. Cells were incubated with VD_3 (at 1 ×MIC) for 12 h, then, (c) the biofilm biomass was scanned with a confocal laser scanning microscope. (d) Effect of VD_3 on cell surface hydrophobicity. (e) Transcription of genes, related to biofilm formation, was quantified by reverse transcription quantitative PCR (RT-qPCR) reaction screening. Samples treated with VD_3 at the concentration of 1 ×MIC were collected at 0 h, 6 h, or 12 h for RNA extraction. Error bars represent standard error. Analysis was carried out by analysis of variance (ANOVA) or unpaired t test: * $P < 0.05$, ** $P < 0.01$, *** $P < 0.001$, **** $P < 0.0001$ compared with the treatment of DMSO (0.8%) or at 0 h. Each experiment was carried out with three biological replicates.

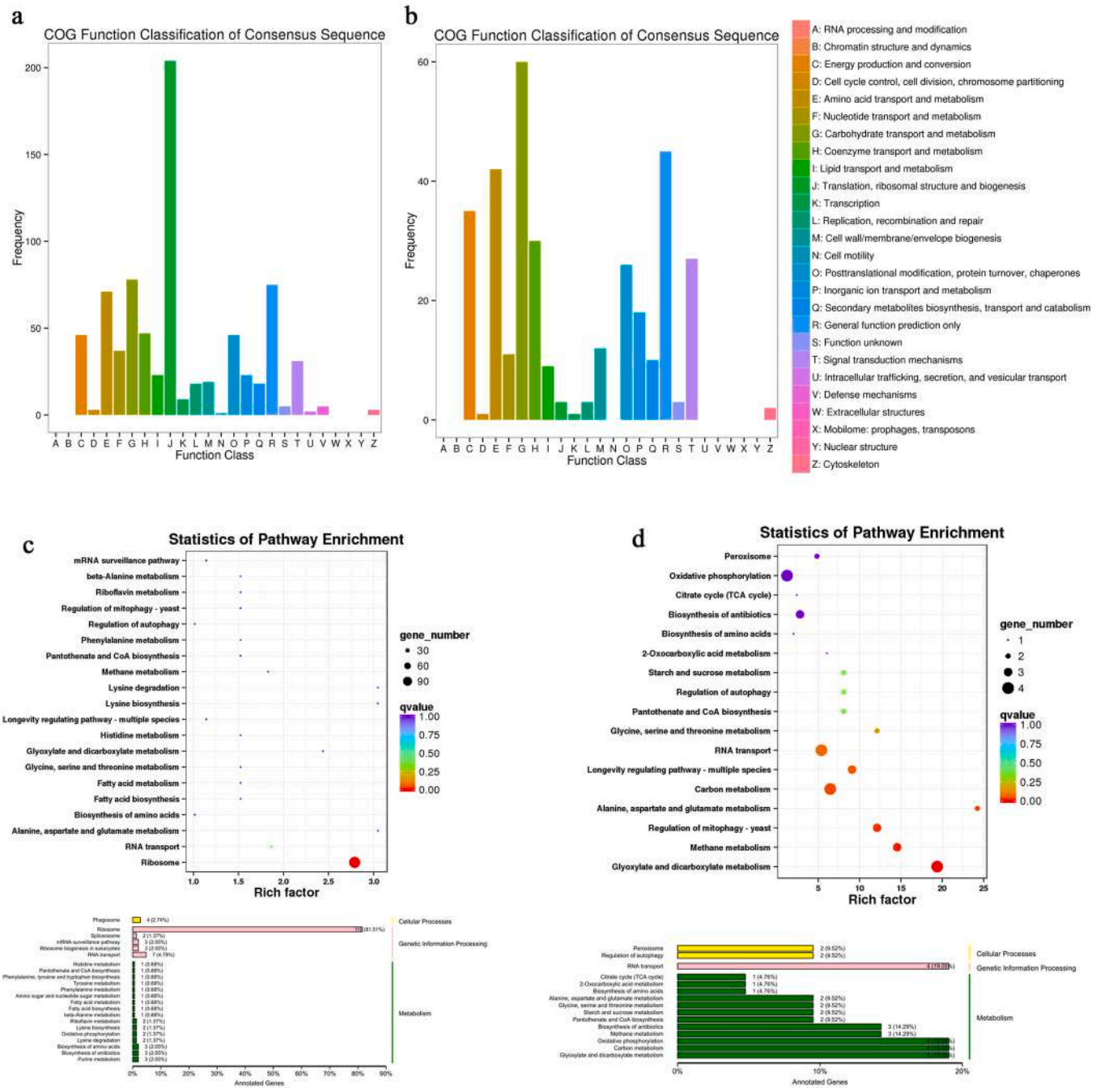

Fig. 4. Transcriptional changes after treatment by VD_3. *C. albicans* were treated with VD_3 at 0.4 mg/mL for 12 h, and then RNA-Seq was performed. There were three biological replicates in each group. Clusters of Orthologous Groups (COG) functional enrichment of (a) up-regulated differential expression genes (DEGs) and (b) down-regulated DEGs. Kyoto Encyclopedia of Genes and Genomes (KEGG) enrichment pathway analysis of (c) up-regulated DEGs and (d) down-regulated DEGs.

the different phases of biofilm formation was investigated (Fig. 3). The results of the CV (Fig. 3a) and XTT assays (Fig. 3b) showed that 1 ×MIC of VD_3 significantly inhibited biofilm formation by *C. albicans* and *C. parapsilosis* during the initial, developmental, and maturation phases. A similar trend was shown with the 2 ×MIC of VD_3 treatment (data not shown). In addition, confocal laser scanning microscopy studies confirmed that VD_3 significantly reduced the biofilm thickness and density (Fig. 3c).

Strains with high cell surface hydrophobicity (CSH) exhibit strong adhesive properties and produce more biofilm (Kumari et al., 2018; Silva-Dias et al., 2015). As shown in Fig. 3d, the CSH of VD_3-treated cells was drastically reduced compared with that of the untreated cells (exposed to DMSO without VD_3). More specifically, compared with the DMSO group (CSH = 73.01 ± 0.038%), the CSH of *C. albicans* was reduced to 14.53 ± 0.084% and 9.85 ± 0.084% at 1 ×MIC and 2 ×MIC VD_3 ($P < 0.001$), respectively. Compared with the CSH of the DMSO group (74.07 ± 0.057%), that of *C. parapsilosis* in the 1 ×MIC (−1.5 ± 0.046%) and 2 ×MIC VD_3 groups (−4.67 ± 0.064%) were significantly lower ($P < 0.001$).

Furthermore, several genes were chosen to explore potential mechanisms of VD_3 action toward biofilm formation. RT-qPCR analysis revealed that the expression levels of hypha-specific genes (*ALS3*, *HWP1*, and *HGT2*) and core biofilm regulator genes (*BCR1* and *NDT80)* were significantly downregulated after treatment with VD_3 at 1 ×MIC (Fig. 3e).

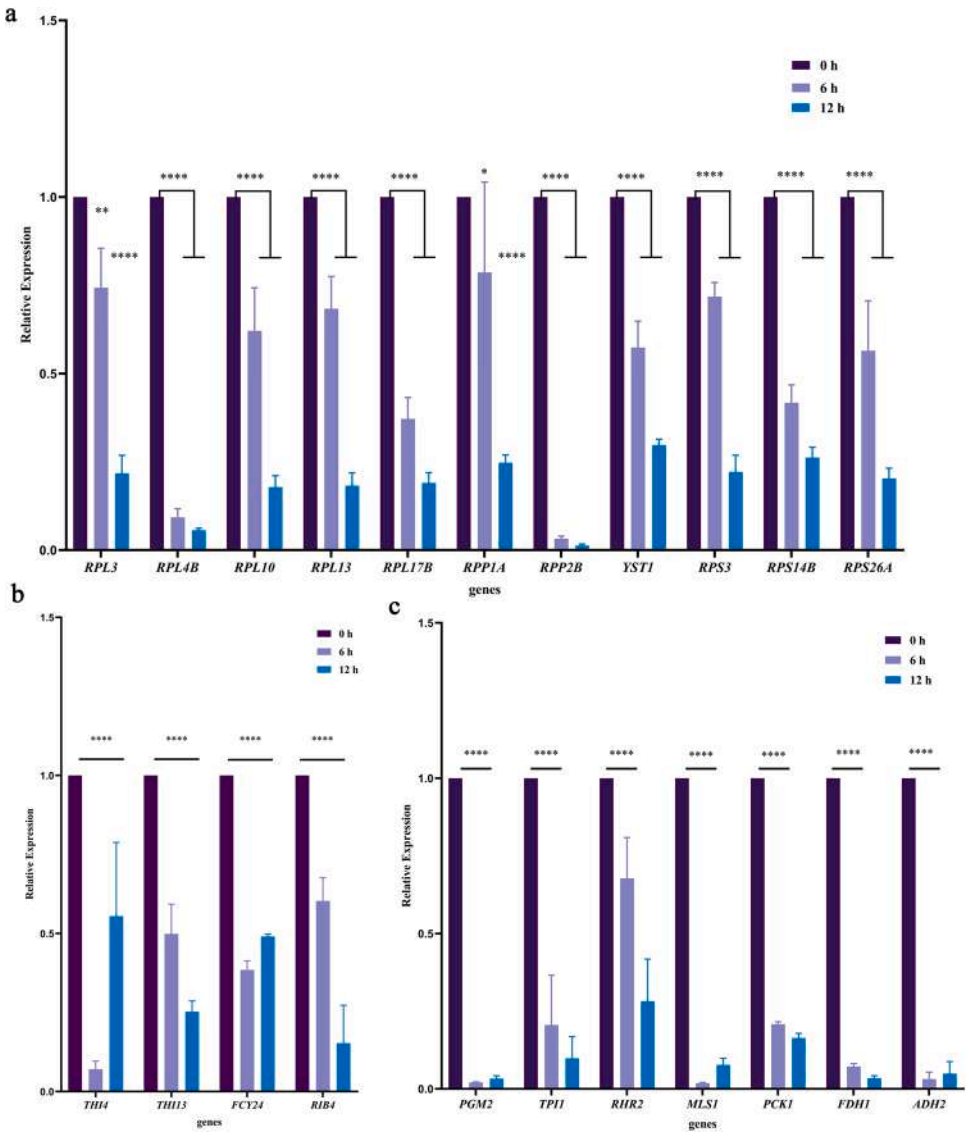

Fig. 5. The expression of genes associated with ribosomal biosynthesis and central metabolism. The expression of genes associated with (a) ribosomal biosynthesis, (b) coenzyme metabolism, and (c) carbon metabolism was evaluated by RT-qPCR. Error bars represent standard error. Analysis was carried out by analysis of variance (ANOVA) or unpaired t test: * $P < 0.05$, ** $P < 0.01$, *** $P < 0.001$, **** $P < 0.0001$, compared with the treatment of 0 h. Each experiment was carried out with three biological replicates.

3.3. The transcriptional response of genes VD_3 involved in ribosome biogenesis and central metabolism to VD_3 treatment

To obtain further insights into the mechanism of VD_3 action on *C. albicans*, the transcriptome changes of *C. albicans* in response to VD_3 treatment were analyzed by RNA-Seq. In total, 1116 genes were differentially expressed in VD_3-treated group (up- and down-regulated genes are 573 and 543, respectively). To understand the functions of the differentially expressed genes (DEGs). Clusters of Orthologous Groups (COG) function classification was used. The up-regulated DEGs were enriched with respect to translation and ribosomal structure and biogenesis (Fig. 4a), whereas the down-regulated DEGs were enriched in terms of carbohydrate transport and metabolism (Fig. 4b).

To further determine the effect of VD_3 on *C. albicans* pathways, Kyoto Encyclopedia of Genes and Genomes (KEGG) pathway enrichment analysis was used for the up-regulated and down-regulated of DEGs. As shown in Fig. 4c, five pathways were enriched in genetic information processing, and 81.51% of the DEGs were functionally annotated in the ribosomal pathway. The down-regulated of DEGs were highly enriched in the central metabolism pathways, including carbon metabolism and glyoxylate and dicarboxylate metabolism, as well as RNA transport (Fig. 4d). Both COG enrichment and KEGG enrichment analysis suggested that DEGs of *C. albicans* treated with VD_3 were enriched in multiple pathways. Furthermore, twenty-two genes were selected to test the accuracy of transcriptomic data. These genes included those involved in ribosome biogenesis (*RPL3*, *RPL4B*, *RPL10*, *RPL13*, *RPL17B*, *RPP1A*, *RPP2B*, *YST1*, *RPS3*, *RPS14*, and *RPS26A*), as well as those involved in coenzyme metabolism (*THI4*, *THI13*, *FCY24* and *RIB4*) and carbon metabolism (*PGM2*, *TPI1*, *RHR2*, *PCK1*, *MLS1*, *FDH1* and *ADH2*). Expression of each of these genes was downregulated after being treated with VD_3 for 6 h or 12 h (Fig. 5). These results indicated that VD_3 affects ribosome biosynthesis and the central metabolism of *C. albicans*.

3.4. VD_3 reduced fungal burden and inflammation in an IAC mouse model

To assess the *in vivo* antifungal effect of VD_3, a murine model of IAC was used. As shown in Fig. 6a, the fungal burden of the liver and kidneys was decreased after three days of daily intraperitoneal treatment with high dose VD_3 (600 μg/kg), although, there was no difference in the fungal burden of the small intestines in mice with or without the VD_3 treatment. After administering VD_3 for 14 days, the high-dose (600 μg/kg) VD_3 treatment significantly decreased the fungal burden of the liver and kidneys as well as the fungal burden in the small intestine, the latter effect also occurring in response to low-VD_3 (60 μg/kg) treatment (Fig. 6b). Histopathological analysis showed that, in the mice of the

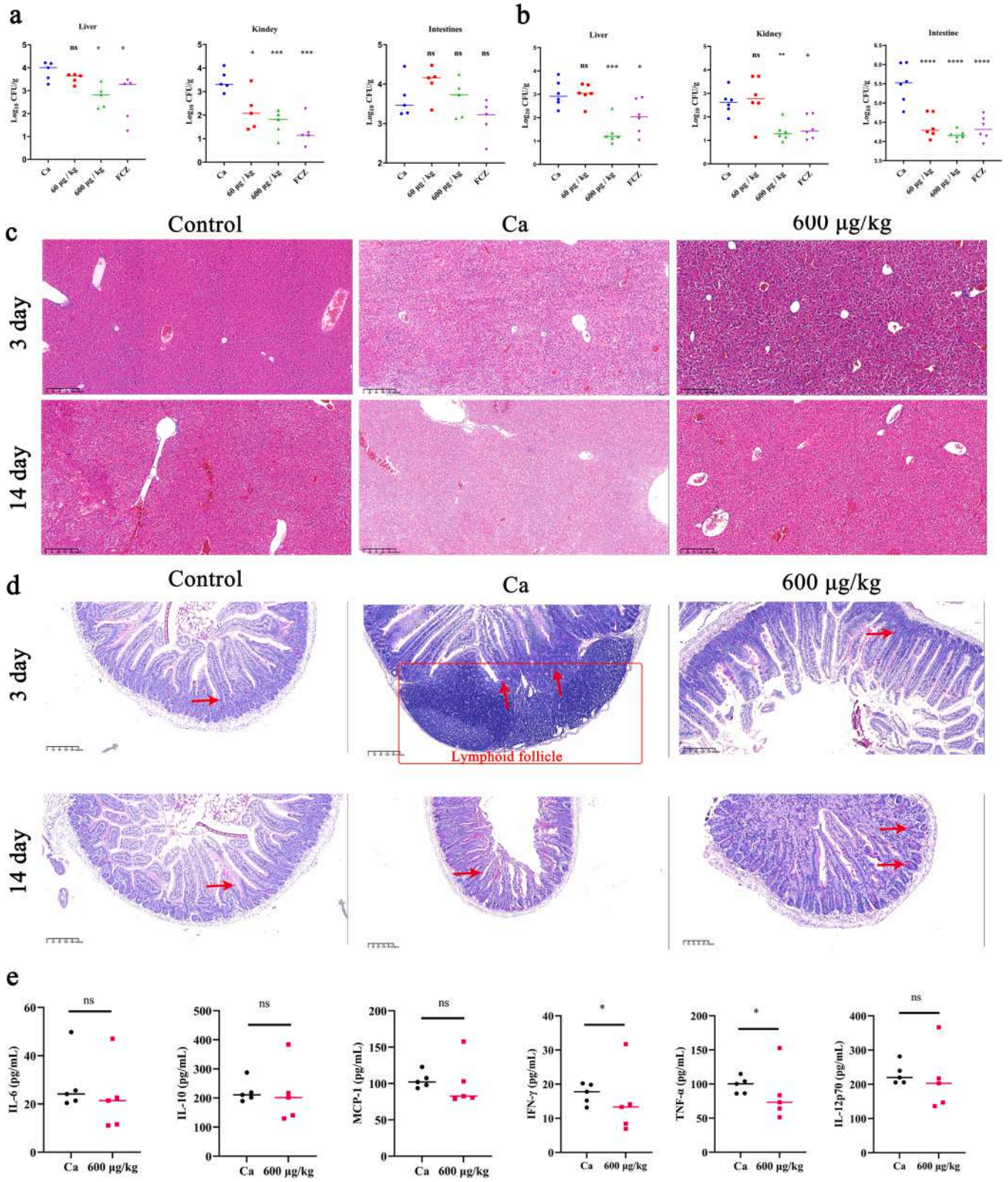

Fig. 6. Antifungal effect of VD_3 *in vivo*. The fungal burden of liver, kidneys and small intestines on the (a) 3rd and (b) 14th day after initial VD_3 administration was determined. (c) Hematoxylin-Eosin (HE) staining of histopathological liver sections. (d) Small intestine histopathological analysis of Periodic Acid-Schiff (PAS) staining. The fungal cells are shown by the red arrow. Lymphoid follicles are shown in the red box. (e) The concentrations of cytokines and chemokines in plasma. Control group: mice injected with normal saline and daily treated with DMSO diluted in normal saline. Ca group: mice injected with *C. albicans* suspended in normal saline and daily treated with DMSO diluted in normal saline. 600 μg/kg group: mice injected with *C. albicans* suspended in normal saline and daily treated with 600 μg/kg of VD_3. Analysis was carried out by analysis of variance (ANOVA) or unpaired t test: Ns: $P > 0.05$, * $P < 0.05$, ** $P < 0.01$, * ** $P < 0.001$, **** $P < 0.0001$, compared with the Ca group. On the 3rd and 14th days, five and six mice, respectively, were sacrificed in each group for the experiments. FCZ: administration of 12 mg/kg of fluconazole per day. CFU: colony forming units.

infection (Ca) group, the liver cells were extensively swollen and the volume was significantly increased, compared with the non-infected control group. Central venous was congested and cytoplasm was loose and light stained. On the other hand, after treatment of infected mice with 600 μg/kg of VD_3 for 14 days, the liver injury was reduced (Fig. 6c) and the small intestine of VD_3-treated mice showed less damage to the intestinal villi and less inflammatory cell infiltration, while the architecture of the small intestine was relatively intact (Fig. 6d).

Next, to test whether there is a change in inflammatory factor concentrations in challenged mice in the presence or absence of VD_3, plasma cytokine and chemokine levels were measured. By the 3rd day of administration, VD_3 treatment had significantly reduced the level of proinflammatory IFN-γ and TNF-α (Fig. 6e), although the decreases in levels of other proinflammatory cytokines (IL-6, IL-12p70, and MCP-1) and anti-inflammatory cytokines (IL-10) were not statistically significant. By the 14th day of administration, VD_3 treatment still did not significantly affect the levels of cytokines (data not shown). These results indicated that VD_3 controls IAC by reducing the levels of proinflammatory IFN-γ and TNF-α during the early stage of administration.

4. Discussion

Repositioning of existing drugs can, to some extent, solve the current problem of resistance to antifungal agents, as well as possibly provide a design idea for the development of drugs with a novel mode of action (Rajasekharan et al., 2019). In the current study, we demonstrated that VD_3 possessed a wide spectrum of activities against *Candida* species, as well as inhibiting biofilm growth and formation *in vitro*. A previous study had reported that the minimum fungistatic concentration of VD_3 against *C. albicans* was 1.58 ± 0.0764 μg/mL, and that the inhibition zone of 100 mg/mL of VD_3 was 12.5 mm (Bouzid et al., 2017). In the present study, the mean MIC of VD_3 against nine *Candida* species was 0.4 mg/mL. Moreover, our group determined that the values of MIC of VD_3 against *A. fumigatus*, *A. flavus*, and *Cryptococcus neoformans* were also 0.4 mg/mL (unpublished data). The difference in VD_3 source and the methods used may contribute to different values of MIC. Furthermore, systematic RNA-Seq and RT-qPCR analysis verified that VD_3 influences carbon metabolism, enzyme biosynthesis, and ribosome biogenesis. The *in vivo* effects observed in the IAC mice model demonstrated that VD_3 had potent antifungal activity. Simlar to previous investigation that the higher daily VD_3 maintenance dose reduced the fungal burden and the production of pro-inflammatory cytokines, as well as achieved the alleviation of inflammatory damage (Mulligan et al., 2017).

Hyphae are crucial for the virulence and invasion of host tissue by *Candida* species (Chen et al., 2020a), and even for immunity evasion (Bain et al., 2014). Fungal cells first colonize the host and form hyphae by producing the extracellular matrix. After that, biofilms are formed. Biofilms on implanted medical devices are an important cause of clinical invasive infection (Nobile and Johnson, 2015). In addition, a biofilm is a crucial virulence factor for the emergence of resistance to drugs. Thus, biofilm inhibitors could become an effective strategy for addressing the problem of drug resistance (Wu et al., 2017). Visually, VD_3 inhibited *C. albicans* and *C. parapsilosis* hyphal formation (Fig. 2), as well as significantly inhibiting the development of biofilm and destroying the mature biofilm (Fig. 3). Furthermore, the ability to achieve biofilm formation is also affected by CSH (Silva-Dias et al., 2015), and the CSH index in *C. albicans* and *C. paraplisosis* decreased after being treated with VD_3 (Fig. 3). We showed that the antifungal and antibiofilm action of VD_3 was associated with transcriptional control of gene expression, with VD_3 treatment downregulating the expression of hypha-related genes (*ALS3*, *HWP1*, and *HGT2*) and biofilm regulators (*BCR1* and *NDT80*).

The cell membrane has been speculated to be a potential target for the antifungal effect of VD_3 (Bouzid et al., 2017). Similarly, calcitriol, the active form of vitamin D, targets the oxidosqualene cyclase of the cell membrane pathway against *C. albicans* and *C. tropicalis* (Rabelo et al., 2019). However, our unpublished data showed that VD_3 did not alter the cell membrane permeability or ergosterol content of *C. albicans*. Transcriptomic profiling revealed that ribosomal biosynthesis and central metabolism may be the potential targets of the anti-*Candida* activity of VD_3 (Figs. 4 and 5). Importantly, 119 of the 164 up-regulated genes in the VD_3-treated fungi are enriched with respect to ribosomal biosynthesis. However, how VD_3 affects the expression of ribosomal biosynthesis-related genes need to be confirmed.

This current study confirms that, broadly speaking, high concentrations of VD_3 are beneficial to recovery from IAC infection. The inhibitory effect of VD_3 towards *C. albicans* in the liver and kidney tissues lasts from the 3rd day to the 14th day (Fig. 6a). The reason for this may be that VD_3 is firstly absorbed by the liver and kidneys, and metabolized to its active form (Christakos et al., 2016) *in vivo*, and then, the active form, calcitriol (1,25 dihydroxycholecalciferol), induces the immune response against fungal infection (Khoo et al., 2011). However, the fungal burden in the small intestine significantly decreased only on the 14th day (Fig. 6b), indicating that the effect of high dose VD_3 on small intestines was indirect. VD_3 achieves anti-inflammatory responses by downregulating the pro-inflammatory cytokines (IFN-γ, IL-6, IL-17, and TNF-α) and upregulating the anti-inflammatory cytokines (Khoo et al., 2011). Similarly, VD_3 reduced the concentrations of TNF-α and IFN-γ (Fig. 6d) in the current study. High-dose VD_3 is detrimental to systemic *Candida* infection (Lim et al., 2015), so we speculate that high-dose VD_3 may play a pleiotropic role in IAC infection. Interestingly. vitamin D supplementation can regulate homeostasis of the gut microbiota (Bashir et al., 2016; Kanhere et al., 2018), which might explain the positive influence of VD_3 on *C. albicans* infection in the small intestine. However, more *in vivo* studies need to be conducted to test this hypothesis.

In summary, we evaluated the antifungal activity of VD_3 against *Candida* species *in vitro* and *in vivo*. Our study demonstrated that VD_3 exhibited an inhibitory effect on hyphal growth and biofilm formation *in vitro* and decreased fungal burden *in vivo* in an IAC mouse model. Further investigations into the mode of action confirmed that VD_3 had multitarget effects against *C. albicans*. Although further experiments are needed to confirm the mechanism underlying these effects, the comprehensive assays carried out in this study revealed that VD_3 has a promising practical value for the treatment of infections caused by *C. albicans*.

Ethics statement

All experimental protocols were approved by the Southwest Medical University Institutional Animal Care and Use Committee (2020540).

CRediT authorship contribution statement

Junwen Lei: Conceptualization, Methodology, Investigation, Formal analysis, Writing – original draft, Writing – review & editing. **Wei Xiao**: Validation. **Jingping Zhang**: Resources, Visualization, Funding acquisition. **Fangyan Liu**: Resources, Visualization, Funding acquisition. **Caiyan Xin**: Resources, Visualization, Funding acquisition. **Bo Zhou**: Resources. **Zhangyong Song**: Supervision, Writing – review & editing, Funding acquisition, Project administration. **Wenbi Chen**: Supervision, Writing – review & editing, Funding acquisition, Project administration. All authors read and approved the manuscript.

Disclosure statement

No potential conflict of interest was reported by the authors.

Data Availability

Data will be made available on request.

Acknowledgments

This research was supported financially by Sichuan Province Administration of Traditional Chinese Medicine (2020JC0129), Technology strategic cooperation project of Luzhou municipal people's government-Southwest Medical University (2020LZXNYDJ38, 2020LZXNYDJ23), Science and Technology Project of Luzhou (2021-JYJ-73), and the Foundation of Southwest Medical University (2020ZRQNA023, 2020ZRQNA039, 2020ZRQNB066, and 2021ZKMS008).

Appendix A. Supporting information

Supplementary data associated with this article can be found in the online version at doi:10.1016/j.micres.2022.127200.

References

Anders, S., Huber, W., 2010. Differential expression analysis for sequence count data. Genome Biol. 11 (10), R106. https://doi.org/10.1186/gb-2010-11-10-r106.

Andes, D., 2019. Has the optimal therapy for invasive candidiasis now been defined. Clin. Infect. Dis. 68 (12), 1990–1992. https://doi.org/10.1093/cid/ciy830.

Andreani, J., Le Bideau, M., Duflot, I., Jardot, P., Rolland, C., Boxberger, M., Wurtz, N., Rolain, J.M., Colson, P., La Scola, B., Raoult, D., 2020. In vitro testing of combined hydroxychloroquine and azithromycin on SARS-CoV-2 shows synergistic effect. Micro Pathog. 145, 104228 https://doi.org/10.1016/j.micpath.2020.104228.

Avram, S., Bologa, C.G., Holmes, J., Bocci, G., Wilson, T.B., Nguyen, D.T., Curpan, R., Halip, L., Bora, A., Yang, J.J., Knockel, J., Sirimulla, S., Ursu, O., Oprea, T.I., 2021. DrugCentral 2021 supports drug discovery and repositioning. Nucleic Acids Res. 49 (D1), D1160–D1169. https://doi.org/10.1093/nar/gkaa997.

Bain, J.M., Louw, J., Lewis, L.E., Okai, B., Walls, C.A., Ballou, E.R., Walker, L.A., Reid, D., Munro, C.A., Brown, A.J., Brown, G.D., Gow, N.A., Erwig, L.P., 2014. *Candida albicans* hypha formation and mannan masking of beta-glucan inhibit macrophage phagosome maturation. mBio 5 (6), e01874. https://doi.org/10.1128/mBio.01874-14.

Bashir, M., Prietl, B., Tauschmann, M., Mautner, S.I., Kump, P.K., Treiber, G., Wurm, P., Gorkiewicz, G., Hogenauer, C., Pieber, T.R., 2016. Effects of high doses of vitamin D_3 on mucosa-associated gut microbiome vary between regions of the human gastrointestinal tract. Eur. J. Nutr. 55 (4), 1479–1489. https://doi.org/10.1007/s00394-015-0966-2.

Bassetti, M., Righi, E., Ansaldi, F., Merelli, M., Scarparo, C., Antonelli, M., Garnacho-Montero, J., Diaz-Martin, A., Palacios-Garcia, I., Luzzati, R., Rosin, C., Lagunes, L., Rello, J., Almirante, B., Scotton, P.G., Baldin, G., Dimopoulos, G., Nucci, M., Munoz, P., Vena, A., Bouza, E., de Egea, V., Colombo, A.L., Tascini, C., Menichetti, F., Tagliaferri, E., Brugnaro, P., Sanguinetti, M., Mesini, A., Sganga, G., Viscoli, C., Tumbarello, M., 2015. A multicenter multinational study of abdominal candidiasis: epidemiology, outcomes and predictors of mortality. Intensive Care Med. 41 (9), 1601–1610. https://doi.org/10.1007/s00134-015-3866-2.

Bassetti, M., Garnacho-Montero, J., Calandra, T., Kullberg, B., Dimopoulos, G., Azoulay, E., Chakrabarti, A., Kett, D., Leon, C., Ostrosky-Zeichner, L., Sanguinetti, M., Timsit, J.F., Richardson, M.D., Shorr, A., Cornely, O.A., 2017. Intensive care medicine research agenda on invasive fungal infection in critically ill patients. Intensive Care Med. 43 (9), 1225–1238. https://doi.org/10.1007/s00134-017-4731-2.

Bouzid, D., Merzouki, S., Bachiri, M., Ailane, S.E., Zerroug, M.M., 2017. Vitamin D_3 a new drug against *Candida albicans*. J. Mycol. Med. 27 (1), 79–82. https://doi.org/10.1016/j.mycmed.2016.10.003.

Carlberg, C., Munoz, A., 2022. An update on vitamin D signaling and cancer. Semin Cancer Biol. 79, 217–230. https://doi.org/10.1016/j.semcancer.2020.05.018.

Cauchie, M., Desmet, S., Lagrou, K., 2017. *Candida* and its dual lifestyle as a commensal and a pathogen. Res. Microbiol 168 (9–10), 802–810. https://doi.org/10.1016/j.resmic.2017.02.005.

Chen, H., Zhou, X., Ren, B., Cheng, L., 2020a. The regulation of hyphae growth in *Candida albicans*. Virulence 11 (1), 337–348. https://doi.org/10.1080/21505594.2020.1748930.

Chen, L., Qu, S., Yang, K., Liu, M., Li, Y.X., Keller, N.P., Zeng, X., Tian, J., 2020b. Perillaldehyde: a promising antifungal agent to treat oropharyngeal candidiasis. Biochem. Pharm. 180, 114201 https://doi.org/10.1016/j.bcp.2020.114201.

Christakos, S., Dhawan, P., Verstuyf, A., Verlinden, L., Carmeliet, G., 2016. Vitamin D: metabolism, molecular mechanism of action, and pleiotropic effects. Physiol. Rev. 96 (1), 365–408. https://doi.org/10.1152/physrev.00014.2015.

Christakos, S., Li, S., De La Cruz, J., Bikle, D.D., 2019. New developments in our understanding of vitamin. Metab. Action Treat. Metab. 98, 112–120. https://doi.org/10.1016/j.metabol.2019.06.010.

Del Rio, M., de la Canal, L., Pinedo, M., Mora-Montes, H.M., Regente, M., 2019. Effects of the binding of a Helianthus annuus lectin to *Candida albicans* cell wall on biofilm development and adhesion to host cells. Phytomedicine 58, 152875. https://doi.org/10.1016/j.phymed.2019.152875.

Hu, W., Zhang, L., Li, M.X., Shen, J., Liu, X.D., Xiao, Z.G., Wu, D.L., Ho, I.H.T., Wu, J.C. Y., Cheung, C.K.Y., Zhang, Y.C., Lau, A.H.Y., Ashktorab, H., Smoot, D.T., Fang, E.F., Chan, M.T.V., Gin, T., Gong, W., Wu, W.K.K., Cho, C.H., 2019. Vitamin D_3 activates the autolysosomal degradation function against *Helicobacter pylori* through the PDIA3 receptor in gastric epithelial cells. Autophagy 15 (4), 707–725. https://doi.org/10.1080/15548627.2018.1557835.

Jiang, L., Fang, M., Tao, R., Yong, X., Wu, T., 2020. Recombinant human interleukin 17A enhances the anti-*Candida* effect of human oral mucosal epithelial cells by inhibiting *Candida albicans* growth and inducing antimicrobial peptides secretion. J. Oral. Pathol. Med. 49 (4), 320–327. https://doi.org/10.1111/jop.12889.

Kanehisa, M., Araki, M., Goto, S., Hattori, M., Hirakawa, M., Itoh, M., Katayama, T., Kawashima, S., Okuda, S., Tokimatsu, T., Yamanishi, Y., 2008. KEGG for linking genomes to life and the environment. Nucleic Acids Res. 36, D480–D484. https://doi.org/10.1093/nar/gkm882.

Kanhere, M., He, J., Chassaing, B., Ziegler, T.R., Alvarez, J.A., Ivie, E.A., Hao, L., Hanfelt, J., Gewirtz, A.T., Tangpricha, V., 2018. Bolus Weekly Vitamin D_3 supplementation impacts gut and airway microbiota in adults with cystic fibrosis: a double-blind, randomized, placebo-controlled clinical trial. J. Clin. Endocrinol. Metab. 103 (2), 564–574. https://doi.org/10.1210/jc.2017-01983.

Khoo, A.L., Chai, L.Y., Koenen, H.J., Kullberg, B.J., Joosten, I., van der Ven, A.J., Netea, M.G., 2011. 1,25-dihydroxyvitamin D_3 modulates cytokine production induced by *Candida albicans*: impact of seasonal variation of immune responses. J. Infect. Dis. 203 (1), 122–130. https://doi.org/10.1093/infdis/jiq008.

Kumamoto, C.A., Gresnigt, M.S., Hube, B., 2020. The gut, the bad and the harmless: *Candida albicans* as a commensal and opportunistic pathogen in the intestine. Curr. Opin. Microbiol 56, 7–15. https://doi.org/10.1016/j.mib.2020.05.006.

Kumari, A., Mankotia, S., Chaubey, B., Luthra, M., Singh, R., 2018. Role of biofilm morphology, matrix content and surface hydrophobicity in the biofilm-forming capacity of various *Candida* species. J. Med Microbiol 67 (6), 889–892. https://doi.org/10.1099/jmm.0.000747.

Lee, A., Prideaux, B., Zimmerman, M., Carter, C., Barat, S., Angulo, D., Dartois, V., Perlin, D.S., Zhao, Y., 2020. Penetration of ibrexafungerp (formerly SCY-078) at the site of infection in an intra-abdominal candidiasis mouse model. Antimicrob. Agents Chemother. 64 (3) https://doi.org/10.1128/AAC.02268-19.

Lee, Y., Puumala, E., Robbins, N., Cowen, L.E., 2021. Antifungal Drug Resistance: Molecular mechanisms in *Candida albicans* and beyond. Chem. Rev. 121 (6), 3390–3411. https://doi.org/10.1021/acs.chemrev.0c00199.

Li, P., Wu, T., Su, X., Shi, Y., 2015. Activation of vitamin D regulates response of human bronchial epithelial cells to *Aspergillus fumigatus* in an autocrine fashion. Mediat. Inflamm. 2015, 208491 https://doi.org/10.1155/2015/208491.

Lim, J.H., Ravikumar, S., Wang, Y.M., Thamboo, T.P., Ong, L., Chen, J., Goh, J.G., Tay, S. H., Chengchen, L., Win, M.S., Leong, W., Lau, T., Foo, R., Mirza, H., Tan, K.S., Sethi, S., Khoo, A.L., Chng, W.J., Osato, M., Netea, M.G., Wang, Y., Chai, L.Y., 2015. Bimodal Influence of vitamin D in host response to systemic *Candida* infection-vitamin D dose matters. J. Infect. Dis. 212 (4), 635–644. https://doi.org/10.1093/infdis/jiv033.

Liu, Y., Lu, J., Sun, J., Zhu, X., Zhou, L., Lu, Z., Lu, Y., 2019. C16-Fengycin a affect the growth of *Candida albicans* by destroying its cell wall and accumulating reactive oxygen species. Appl. Microbiol Biotechnol. 103 (21–22), 8963–8975. https://doi.org/10.1007/s00253-019-10117-5.

Livak, K.J., Schmittgen, T.D., 2001. Analysis of relative gene expression data using real-time quantitative PCR and the 2(-Delta Delta C(T)) Method. Methods 25 (4), 402–408. https://doi.org/10.1006/meth.2001.1262.

Logan, C., Martin-Loeches, I., Bicanic, T., 2020. Invasive candidiasis in critical care: challenges and future directions. Intensive Care Med 46 (11), 2001–2014. https://doi.org/10.1007/s00134-020-06240-x.

Meza-Meza, M.R., Ruiz-Ballesteros, A.I., de la Cruz-Mosso, U., 2020. Functional effects of vitamin D: from nutrient to immunomodulator. Crit. Rev. Food Sci. Nutr. 1–21. https://doi.org/10.1080/10408398.2020.1862753.

Montravers, P., Leroy, O., Eckmann, C., 2015. Intra-abdominal candidiasis: it's still a long way to get unquestionable data. Intensive Care Med 41 (9), 1682–1684. https://doi.org/10.1007/s00134-015-3894-y.

Mora, J.R., Iwata, M., von Andrian, U.H., 2008. Vitamin effects on the immune system: vitamins A and D take centre stage. Nat. Rev. Immunol. 8 (9), 685–698. https://doi.org/10.1038/nri2378.

Mulligan, J.K., Pasquini, W.N., Carroll, W.W., Williamson, T., Reaves, N., Patel, K.J., Mappus, E., Schlosser, R.J., Atkinson, C., 2017. Dietary vitamin D_3 deficiency exacerbates sinonasal inflammation and alters local 25(OH)D_3 metabolism. PLoS One 12 (10), e0186374. https://doi.org/10.1371/journal.pone.0186374.

Nguyen, N.L., Pilewski, J.M., Celedon, J.C., Mandalapu, S., Blanchard, M.L., DeRicco, A., Hartigan, E., Alcorn, J.F., Kolls, J.K., 2015. Vitamin D supplementation decreases *Aspergillus fumigatus* specific Th2 responses in CF patients with aspergillus sensitization: a phase one open-label study. Asthma Res Pr. 1. https://doi.org/10.1186/s40733-015-0003-5.

Nobile, C.J., Johnson, A.D., 2015. *Candida albicans* biofilms and human disease. Annu Rev. Microbiol 69, 71–92. https://doi.org/10.1146/annurev-micro-091014-104330.

Pappas, P.G., Kauffman, C.A., Andes, D., Benjamin, D.K., Jr., Calandra, T.F., Edwards, J. E., Jr., Filler, S.G., Fisher, J.F., Kullberg, B.J., Ostrosky-Zeichner, L., Reboli, A.C., Rex, J.H., Walsh, T.J., Sobel, J.D., Infectious Diseases Society of A, 2009. Clinical practice guidelines for the management of candidiasis: 2009 update by the Infectious Diseases Society of America. Clin. Infect. Dis. 48 (5), 503–535. https://doi.org/10.1086/596757.

Pappas, P.G., Lionakis, M.S., Arendrup, M.C., Ostrosky-Zeichner, L., Kullberg, B.J., 2018. Invasive candidiasis. Nat. Rev. Dis. Prim. 4, 18026. https://doi.org/10.1038/nrdp.2018.26.

Rabelo, V.W., Viegas, D.J., Tucci, E.M.N., Romeiro, N.C., Abreu, P.A., 2019. Virtual screening and drug repositioning as strategies for the discovery of new antifungal inhibitors of oxidosqualene cyclase. J. Steroid Biochem Mol. Biol. 185, 189–199. https://doi.org/10.1016/j.jsbmb.2018.09.001.

Rajasekharan, S.K., Lee, J.H., Lee, J., 2019. Aripiprazole repurposed as an inhibitor of biofilm formation and sterol biosynthesis in multidrug-resistant *Candida albicans*. Int J. Antimicrob. Agents 54 (4), 518–523. https://doi.org/10.1016/j.ijantimicag.2019.05.016.

Rajendran, R., Borghi, E., Falleni, M., Perdoni, F., Tosi, D., Lappin, D.F., O'Donnell, L., Greetham, D., Ramage, G., Nile, C., 2015. Acetylcholine protects against *Candida albicans* infection by inhibiting biofilm formation and promoting hemocyte function in a galleria mellonella infection model. Eukaryot. Cell 14 (8), 834–844. https://doi.org/10.1128/EC.00067-15.

Silva-Dias, A., Miranda, I.M., Branco, J., Monteiro-Soares, M., Pina-Vaz, C., Rodrigues, A. G., 2015. Adhesion, biofilm formation, cell surface hydrophobicity, and antifungal planktonic susceptibility: relationship among *Candida* spp. Front Microbiol. 6, 205. https://doi.org/10.3389/fmicb.2015.00205.

Thangamani, S., Maland, M., Mohammad, H., Pascuzzi, P.E., Avramova, L., Koehler, C. M., Hazbun, T.R., Seleem, M.N., 2017. Repurposing approach identifies auranofin with broad spectrum antifungal activity that targets Mia40-Erv1 pathway. Front Cell Infect. Microbiol. 7, 4. https://doi.org/10.3389/fcimb.2017.00004.

Wu, S., Wang, Y., Liu, N., Dong, G., Sheng, C., 2017. Tackling fungal resistance by biofilm inhibitors. J. Med. Chem. 60 (6), 2193–2211. https://doi.org/10.1021/acs.jmedchem.6b01203.

Xu, K., Wang, J.L., Chu, M.P., Jia, C., 2019. Activity of coumarin against *Candida albicans* biofilms. J. Mycol. Med. 29 (1), 28–34. https://doi.org/10.1016/j.mycmed.2018.12.003.

Zhang, Q., Liu, F., Zeng, M., Mao, Y., Song, Z., 2021. Drug repurposing strategies in the development of potential antifungal agents. Appl. Microbiol. Biotechnol. 105 (13), 5259–5279. https://doi.org/10.1007/s00253-021-11407-7.